Time Domain Flutter Analysis of Cascades Using a Full-Potential Solver

Milind A. Bakhle,* T. S. R. Reddy,† and Theo G. Keith Jr.‡
University of Toledo, Toledo, Ohio 43606

A time domain approach is used to determine the aeroelastic stability of a cascade of blades. The structural model for each blade is a typical section with two degrees of freedom. The aerodynamic model is unsteady, two-dimensional, full-potential flow through the cascade of airfoils. The unsteady equations of motion for the structure and the fluid are integrated simultaneously in time starting with a steady flowfield and a small initial disturbance applied to the airfoils. Each blade is allowed to move independently, and the motion of all blades is analyzed to determine the aeroelastic stability of the cascade. The airfoil section and structural parameters are selected to be representative of a propfan. The results are compared with those from a separate frequency domain analysis based on the same aerodynamic model. Good agreement between the results is observed. Since the present calculations are meant to validate the time domain approach, only linear examples are considered. However, with the time domain approach, it is possible to consider nonlinear structural models and nonlinear force-displacement relations. Because of this, the method allows a more realistic simulation of the motion of the fluid and the cascade blades that should lead to a better physical understanding.

Nomenclature

a	= sonic velocity
a_1,b_1,c_1,w_1	= amplitude, phase, damping, and frequency parameters in Eq. (10)
b	= airfoil semichord
$C_L,\overline{C_L}$	= lift coefficient and steady value of lift coefficient
$C_M,\overline{C_M}$	= moment coefficient about elastic axis and steady value
c	= airfoil chord
h	= plunging displacement, normal to airfoil chord
I_α	= moment of inertia about elastic axis
Im{ }	= imaginary part of { }
i	= imaginary unit, $\sqrt{-1}$
K_h,K_α	= spring constants for plunging and pitching
k_c	= reduced frequency, $\omega c/M_\infty a_\infty$
$l_{hh},l_{h\alpha},l_{\alpha h},l_{\alpha\alpha}$	= frequency domain aerodynamic coefficients, Eq. (5)
M	= Mach number
m	= mass of typical section
N	= number of blades in the cascade
Q_h,Q_α	= lift and moment about elastic axis
r_α	= radius of gyration about elastic axis, $\sqrt{I_\alpha/mb^2}$
Re{ }	= real part of { }
S_α	= static unbalance
s/c	= gap-to-chord ratio
t	= time
u,v	= fluid velocity in x and y directions
V^*	= reduced velocity, $M_\infty a_\infty/b\omega_\alpha$
x,y	= Cartesian coordinates
x_α	= distance between elastic axis and center of mass, S_α/mb
α	= pitching displacement about elastic axis
γ	= ratio of specific heats
θ	= stagger angle
μ	= mass ratio, $m/\pi\rho_\infty b^2$
ρ	= fluid density
σ	= interblade phase angle
τ	= nondimensional time, $a_\infty t/c$
$\Delta\tau$	= time step
ϕ	= velocity potential
ω	= oscillation frequency
ω_h	= uncoupled natural frequency for bending (plunging), $\sqrt{K_h/m}$
ω_α	= uncoupled natural frequency for torsion (pitching), $\sqrt{K_\alpha/I_\alpha}$
Ω	= nondimensional frequency, $\omega c/a_\infty$

Subscripts and Supercripts

$(\dot{})$	= d( )/dt
$(\,)'$	= d( )/dτ
0	= amplitude of harmonic motion
∞	= evaluated at inlet section

Presented as Paper 90-0984 at the AIAA/ASME/ASCE/AHS/ASC 31st Structures, Structural Dynamics, and Materials Conference, Long Beach, CA, April 2-4, 1990; received April 17, 1990; revision received Aug. 31, 1990; accepted for publication Sept. 14, 1990.

*Research Associate, Department of Mechanical Engineering. Student Member AIAA.

†Senior Research Associate, Department of Mechanical Engineering. Member AIAA.

‡Distinguished Professor, Department of Mechanical Engineering. Associate Fellow AIAA.

Introduction

In recent years, there has been renewed interest in the use of turboprop engines for more efficient transport. Research programs have been under way[1] to develop advanced turboprops that combine the efficiency of conventional propellers with the high cruise speeds of turbojets. The result of this research is a propfan that operates at high subsonic cruise Mach numbers. However, the thin, twisted, and highly swept blades of the propfan have shown a susceptibility to a coupled bending-torsion flutter in attached flow, i.e., classical flutter.[2]

The traditional approach in flutter calculations of bladed disks (stators and rotors) has been to apply frequency domain analysis.[3] In this approach, the blade motions are assumed to be harmonic functions of time with a constant phase lag between adjacent blades. The equations of motion then reduce to an eigenvalue probelm; the eigenvalues determine stability. This analysis is restricted to linear structural equations and aerodynamic forces that are linearly dependent on the displacements. The unsteady aerodynamic forces used in such an analysis are typically based on classical linearized potential

theory[4-7] that neglects the effects of blade loading due to thickness, camber, and angle of attack but allows the use of efficient semianalytical solution methods.

Over the last decade, researchers[8-12] have developed unsteady aerodynamic linerarizations that include the effects of real blade geometry, mean blade loading, and transonic flow. In these analyses, the unsteady flow is regarded as a small-amplitude perturbation about a nonuniform steady flow. The steady flow is governed by nonlinear equations, whereas the unsteady flow is governed by linear equations with variable coefficients that depend on the steady flow. A review of this type of linearization can be found in Ref. 13.

In the present study, the unsteady full-potential equation is used as the basis of a model that is capable of representing flows over a wide Mach number range from low subsonic to supersonic, including transonic flows with weak shocks.[14] The aerodynamic model fully accounts for blade thickness and camber and angle-of-attack effects. Since the computational method used to solve the full-potential equation is based on a time-marching algorithm, it is natural to consider a time domain flutter analysis method. The time domain method of flutter analysis, which is in widespread use in fixed-wing aeroelasticity,[15,16] is based on the simultaneous integration in time of the equations of motion for the structure and the fluid.[17] The time domain method is not restricted to linear structural models and does not require the assumption of a linear relation between aerodynamic loads and blade displacements. The time domain approach allows an accurate representation of the onset of flutter in a bladed disk when it encounters some nonuniformity in an otherwise uniform inlet flow.

In the present study, the simultaneous time integration method is used to calculate the flutter speed for a two-dimensional cascade of airfoils. Separate frequency domain flutter calculations are also made using the same time-marching aerodynamic solver with harmonically oscillating blades. The validity of the time domain method is demonstrated, at least for linear flows. Two examples are considered. In the first, each blade is assumed to have only a pitching degree of freedom. In the second example, each blade has two degrees of freedom. The airfoil shape, the cascade parameters, and the parameters in the structural model that are used in the second example are representative of the SR5 propfan.[2]

Formulation

The aerodynamic and aeroelastic models used are described briefly in the following subsections.

Aerodynamic Model

The aerodynamic model is based on the unsteady, two-dimensional, full-potential equation. The governing equation for irrotational, isentropic flow written in conservative form is

$$\frac{\partial \rho}{\partial t} + \frac{\partial(\rho u)}{\partial x} + \frac{\partial(\rho v)}{\partial y} = 0 \tag{1}$$

where

$$u = \frac{\partial \phi}{\partial x}$$

$$v = \frac{\partial \phi}{\partial y}$$

$$\frac{\rho}{\rho_\infty} = \left(1 + \frac{(\gamma-1)}{2}\left\{M_\infty^2 - \left[2\frac{\partial \phi}{\partial t} + (u^2+v^2)\right]/a_\infty^2\right\}\right)^{1/(\gamma-1)}$$

Here ϕ is the velocity potential; ρ_∞, a_∞, and M_∞ are the density, sonic velocity, and Mach number, respectively, all evaluated at the inlet section.

The governing equation is transformed to the computational plane where it is discretized and solved using a finite-volume scheme. The method of solution is a time-marching scheme that uses approximate factorization at each time level with quasi-Newton iterations to maintain time accuracy.

The governing equation is solved as an initial-boundary value problem. For steady calculations, a uniform flowfield is used as the initial condition; for unsteady calculations, the steady flowfield is used as the initial condition. The airfoil surfaces are treated as impermeable; that is, the normal velocity of the fluid relative to the airfoil surface is zero. This condition of flow tangency is imposed at the instantaneous position of the airfoil at each time step. To do this, a new grid that conforms to the airfoil surfaces is generated at each time step. Blade motions are thus fully accounted for using moving grids. Wake positions are prescribed in advance; continuity of pressure and normal velocity is then enforced across the wakes. At the inlet and exit boundaries, characteristic boundary conditions are used; the one-dimensional Riemann invariant corresponding to the incoming characteristic is prescribed at these boundaries based on the specified inlet/exit conditions. The Riemann-invariant boundary conditions allow acoustic waves to pass through without significant reflections and serve as nonreflecting boundary conditions. Finally, periodicity conditions are imposed across the cascade. Additional details concerning the aerodynamic model can be found in Refs. 14 and 18.

Aeroelastic Model

The aeroelastic model for the cascade consists of a typical section with two degrees of freedom (bending and torsion) for each blade. Structural damping is not considered at present, although it could be included with very little additional complication. The equations of motion for each blade of the cascade have the following form:

$$m\ddot{h} + S_\alpha \ddot{\alpha} + K_h h = Q_h \tag{2a}$$

$$S_\alpha \ddot{h} + I_\alpha \ddot{\alpha} + K_\alpha \alpha = Q_\alpha \tag{2b}$$

The preceding equations can be written in matrix notation as

$$[M]\{\ddot{X}\} + [K]\{X\} = \{F\} \tag{3}$$

where

$$[M] = \begin{bmatrix} 1 & x_\alpha \\ x_\alpha & r_\alpha^2 \end{bmatrix}, \qquad [K] = \begin{bmatrix} \omega_h^2 & 0 \\ 0 & r_\alpha^2 \omega_\alpha^2 \end{bmatrix}$$

$$\{X\} = \begin{Bmatrix} h/b \\ \alpha \end{Bmatrix}, \qquad \{F\} = \begin{Bmatrix} Q_h/mb \\ Q_\alpha/mb^2 \end{Bmatrix}$$

where ω_h and ω_α are the uncoupled natural frequencies for bending and torsion, respectively; x_α is the distance between the elastic axis and center of mass in semichord units; x_α is the radius of gyration about the elastic axis in semichord units; and b is the airfoil semichord.

Flutter Analysis

The methods of flutter analysis in the frequency domain and the time domain are described briefly in the following subsections.

Frequency Domain Method

In the frequency domain method, the blade displacements are assumed to be harmonic functions of time and blade number:

$$\{X\} = \{X_0\} e^{i(\omega t + n\sigma)}, \qquad n = 0, 1, 2, \ldots, N-1 \tag{4}$$

where N is the number of blades in the cascade, and n is a blade index. Further, the aerodynamic loads are assumed to be linear functions of the displacements:

$$Q_h = \pi \rho_\infty b^3 \omega^2 [l_{hh}(h/b) + l_{h\alpha}(\alpha)] \tag{5a}$$

$$Q_\alpha = \pi\rho_\infty b^4\omega^2[l_{\alpha h}(h/b) + l_{\alpha\alpha}(\alpha)] \tag{5b}$$

or

$$\{F\} = \left(\frac{\omega^2}{\mu}\right)[A]\{X\}$$

where μ is the mass ratio and $[A]$ is the matrix of frequency domain unsteady aerodynamic coefficients:

$$[A] = \begin{bmatrix} l_{hh} & l_{h\alpha} \\ l_{\alpha h} & l_{\alpha\alpha} \end{bmatrix}$$

The aeroelastic equations yield an eigenvalue problem (for each blade):

$$\left([K]^{-1}[M] + \frac{1}{\mu}[K]^{-1}[A]\right)\{X\} = \frac{1}{\omega^2}\{X\} \tag{6}$$

For a tuned cascade, in which all blades are identical (and thus have identical values of structural parameters), the same eigenvalue problem is obtained for each blade. Hence, it is sufficient to solve this problem for just one of the blades. The two eigenvalues obtained from the solution are generally complex. The imaginary part of the eigenvalue determines the stability of the system; the system is said to flutter if the imaginary part of either eigenvalue is nonpositive.

The frequncy domain aerodynamic coefficients (l_{hh}, $l_{h\alpha}$, etc.) are obtained from the unsteady full-potential solver as follows. To begin, a steady flowfield is obtained for the given cascade geometry (stagger angle θ and gap-to-chord ratio s/c) and specified inlet Mach number M_∞. Starting with this steady flowfield, the airfoil motions are specified as sinusoidal variations in time with a fixed phase angle between adjacent blades:

Plunging:

$$h = h_0 \sin(k_c M_\infty \tau + n\sigma)$$

Pitching:

$$\alpha = \alpha_0 \sin(k_c M_\infty \tau + n\sigma), \qquad n = 0, 1, 2, \ldots, N-1$$

where k_c is the reduced frequency based on airfoil chord and τ is a nondimensional time.

After the initial transients have decayed, the lift and moment coefficients show a sinusoidal variation. The variation of the lift and moment coefficients is recorded as a function of time. This time history is then decomposed into Fourier components to obtain the complex frequency domain aerodynamic coefficients. This procedure is done separately for each blade motion—plunging and pitching. It must then be repeated for each possible value of interblade phase angle; however, in practice, only a few are investigated. For a cascade with N blades, the values of interblade phase angle at which flutter can occur are given[19] as

$$\sigma = 2\pi j/N, \qquad j = 0, 1, 2, \ldots, N-1 \tag{7}$$

In general, computations are made using a number of blade passages equal to the number of blades in the cascade. Periodic boundary conditions are applied at the upper and lower boundaries of the cascade. However, there are some situations when it is possible to reduce the number of passages used in the calculations. For unsteady flows in which all the blades have the same periodic motion (zero interblade phase angle), blade-to-blade periodicity of flow variables exists naturally. Hence, only a single blade passage is used in the computations; periodicity conditions are imposed at the upper and lower boundaries of the blade passage. For periodic motions with the a nonzero interblade phase angle, it is occasionally possible to reduce the number of blade passages used in the calculations depending on the value of the interblade phase angle. For instance, computations with the phase angle $\sigma = 180$ deg can be made in two passages, computations with phase angles $\sigma = 120$ or 240 deg can be made in three passages, and so on. Except for the special cases of the type mentioned here, it is necessary to use a number of passages equal to the number of blades in the cascade (N). The preceding discussion is applicable only when the motion of the blades is known in advance. In the time domain method, since the motion of the blades is not known beforehand, it is necessary to always include all N passages in the calculations.

For small amplitudes of motion, the aerodynamic forces C_L and C_M are linearly related to the amplitude of motion. The present calculations are restricted to this linear range of aerodynamic response. To ascertain this, selected calculations were repeated with the amplitude of motion reduced in half. No change in the aerodynamic derivatives (l_{hh}, $l_{h\alpha}$, etc.) was observed; this indicated that the amplitudes selected were small enough to ensure a linear aerodynamic response.

Time Domain Method

In the time domain method, the equations of motion for all blades are integrated in time. The initial conditions are the steady flowfield and a small initial disturbance applied to the blades in the cascade. The aeroelastic equation for a single blade can be rewritten as

$$[M]\{X\}'' + \left(\frac{2M_\infty}{V^*\omega_\alpha}\right)^2[K]\{X\} = \{F\} \tag{8}$$

where the primes indicate differentiation with respect to nondimensional time τ and V^* is the reduced velocity; the aerodynamic loads are expressed in terms of the lift and moment coefficients C_L and C_M, respectively; and the steady values $\overline{C_L}$ and $\overline{C_M}$ are subtracted out:

$$\{F\} = \left(\frac{4M_\infty^2}{\pi\mu}\right)\begin{Bmatrix} 2(C_L - \overline{C_L}) \\ (C_M - \overline{C_M}) \end{Bmatrix}$$

The aeroelastic equations are integrated by a method of constant average acceleration[20]; this is sometimes referred to as the trapezoidal rule. Equation (8) is discretized as follows:

$$[M]\{X\}''_{\tau+\Delta\tau} + \left(\frac{2M_\infty}{V^*\omega_\alpha}\right)^2[K]\{X\}_{\tau+\Delta\tau} = \{F\}_\tau \tag{9}$$

where the subscripts τ and $\tau + \Delta\tau$ denote time levels and it is assumed that

$$\{X\}'_{\tau+\Delta\tau} = \{X\}'_\tau + \left(\frac{\Delta\tau}{2}\right)(\{X\}''_\tau + \{X\}''_{\tau+\Delta\tau})$$

$$\{X\}_{\tau+\Delta\tau} = \{X\}_\tau + \Delta\tau\{X\}'_\tau + \left(\frac{\Delta\tau^2}{2}\right)(\{X\}''_\tau + \{X\}''_{\tau+\Delta\tau})$$

The initial conditions required to begin the time-integration procedure are described in the following section together with the results.

A two-dimensional cascade aeroelasticity program, based on the formulations presented earlier, has been developed. A flowchart of the program setup is shown in Fig. 1.

Results

Results are presented for two examples. The first one is a single-degree-of-freedom (pitching) example, which is similar to a case considered in Refs. 18 and 21. The second example is a two-degree-of-freedom case with geometric and structural parameters corresponding to the SR5 profan.[22] Results from both frequency domain and time domain methods are presented for these two examples.

Single-Degree-of-Freedom Example

A cascade with nine blades is considered; the stagger angle θ is 45 deg, and the gap-to-chord ratio s/c is 1.0. The struc-

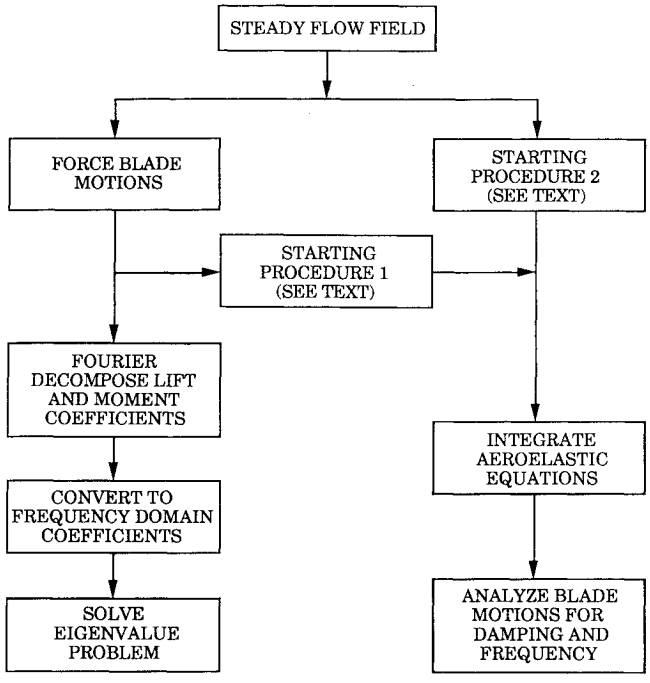

Fig. 1 Setup of computational aeroelasticity program.

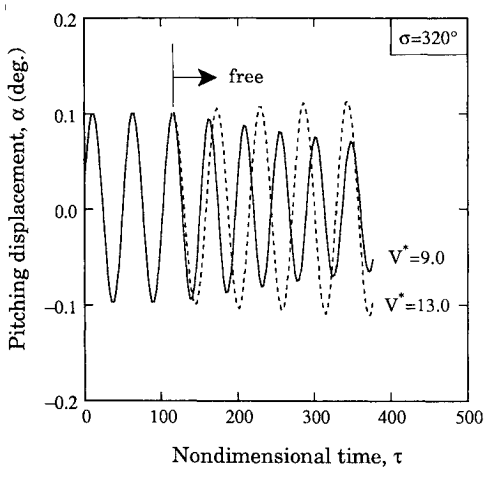

Fig. 2 First starting procedure, blade motions for reduced velocity $V^* = 9.0$ and 13.0.

tural model for each blade is simplified to a single-degree-of-freedom pitching airfoil with elastic axis at the leading edge. The mass ratio is $\mu = 100$, and the radius of gyration is $r_\alpha = 1$. The airfoil is a flat plate, and the Mach number is 0.5 at the inlet. The H grid used in the calculations has 41 points in the streamwise direction and 21 points in the transverse direction in each blade passage; the grid points are distributed nonuniformly in both directions. The nondimensional time step used is 0.06.

To begin, a frequency domain solution is obtained. For this single-degree-of-freedom system, the stability is determined entirely by the sign of the imaginary part (component out of phase with motion) of the moment coefficient; flutter is said to occur if $\mathrm{Im}\{l_{\alpha\alpha}\} \geq 0$. For a cascade with nine blades, the values of interblade phase angle that can be present at flutter are 0, 40, 80, . . . , 320 deg [see Eq. (7)]. A reduced frequency k_c is selected and the airfoils are forced in a pitching motion. The moment coefficient is calculated at each time step. A Fourier decomposition of the moment coefficient variation yields a complex vlaue of $l_{\alpha\alpha}$. This is repeated for each of the

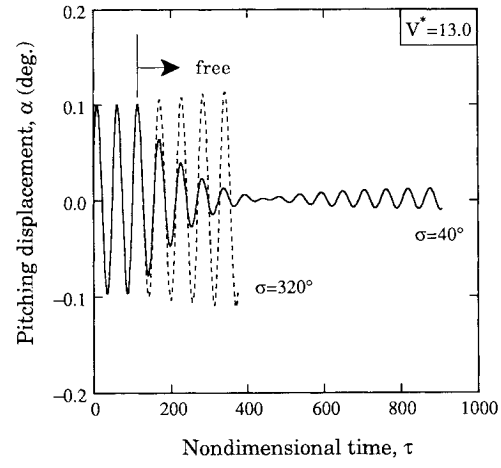

Fig. 3 First starting procedure, blade motions for phase angle of forced motion $\sigma = 40$ and 320 deg.

nine values of σ. The highest value (lowest negative value) of $\mathrm{Im}\{l_{\alpha\alpha}\}$ corresponds to the most unstable (critical) phase angle. If all the values of $\mathrm{Im}\{l_{\alpha\alpha}\}$ are negative, then the system is stable at the selected k_c. A lower value of k_c is selected, and the process is repeated until the $\mathrm{Im}\{l_{\alpha\alpha}\}$ corresponding to the critical interblade phase angle changes sign from negative to positive. For the problem considered here, the value of reduced frequency at flutter is $k_c = 0.238$, the critical phase angle is $\sigma = 320$ deg, and the frequency ratio is $\omega/\omega_\alpha = 1.33$.

Next, a time domain solution is obtained for the same example. Two different starting procedures are considered.

In the first procedure,[23] all the blades are oscillated in a sinusoidal motion with a specified interblade phase angle. The blade displacements and velocities and the flow variables at the end of the two cycles of oscillations are used as the initial conditions for the time-integration procedure. A reduced velocity V^* is selected and the aeroelastic equations are integrated in time to obtain the blade motions. The amplitude of oscillations grows or decays depending on the value of reduced velocity V^*. In this procedure, the blade motion is initially confined to the specific phase angle selected in the initial condition. Concequently, the stability of the cascade can be determined for the phase angle selected in the starting procedure.

Figure 2 illustrates this starting procedure for two values of reduced velocity, $V^* = 9.0$ and 13.0. The interblade phase angle of the forced motion is $\sigma = 320$ deg, which is the critical value obtained in the frequency domain analysis. Only the motion of one blade is shown. The motions of the remaining eight blades are similar, except that adjacent blades are displaced along the time axis by a time interval corresponding to 320 deg. It can be seen that $V^* = 9.0$ results in a decay in the amplitude of blade oscillations, whereas $V^* = 13.0$ leads to growing oscillations; the value of reduced velocity for neutral stability lies somewhere between these values.

To investigate the stability and behavior at some other interblade phase angle, calculations were started from a forced motion with $\sigma = 40$ deg; a frequency domain analysis has shown that this phase angle corresponds to a stable condition. Figure 3 illustrates the results of the first starting procedure for two values of interblade phase angle (of forced motion) $\sigma = 40$ and 320 deg; the reduced velocity is $V^* = 13.0$. Once again, the response of only one of the nine blades is shown. The response for $\sigma = 320$ deg, shown earlier in Fig. 2, is repeated for comparison purposes. The blade motion for $\sigma = 40$ deg initially shows an oscillatory decay. However, at large values of nondimensional time, the amplitude of oscillations is seen to grow. A careful study of the results reveals the following. The blade motion was initially forced with a phase angle of 40 deg. After being released, the blade motion shows

the same phase angle for some time; since this phase angle corresponds to stable motion, the amplitude decays. Then a transient behavior is observed near $\tau = 450$. Following this, the blade motion changes to a phase angle of 320 deg; since $\sigma = 320$ deg represents an unstable condition, the amplitude of oscillations grows. This clearly shows that the short time response of the blades is dominated by the phase angle used in the initial conditions. The long time response, on the other hand, is dominated by the most unstable phase angle.

A second starting procedure was developed to take advantage of the observation that the least stable phase angle mode dominates the long-term response, irrespective of which phase angle is used in the initial conditions. In this second procedure, the blades are not oscillated in a forced motion. Instead, initial displacements and velocities are zero for all but one blade; the center blade is given a small initial velocity and a zero initial displacement. Unlike the first procedure, these initial conditions do not correspond to a sinusoidal motion with a specific interblade phase angle. Consequently, the blade displacements obtained from this procedure can be used to determine the stability of the cascade for all possible interblade phase angles since no specific phase angle is used in the starting procedure. This procedure eliminates the need to check the stability for each phase angle separately and is therefore preferable to the first procedure.

To demonstrate the second starting procedure, calculations are made with two values of reduced velocity $V^* = 9.0$ and 13.0. Only one of the nine blades (the center blade) is given a small initial velocity. All the other initial blade displacements and velocities are zero. The response of the blade with the nonzero initial velocity is shown in Fig. 4. The motion of the other eight blades is not shown due to space limitations. Instead, the displacement of each blade is curve fitted as a function of time during the last two cycles of oscillation. The model used in the curve fit is

$$\alpha = a_1 e^{c_1 \tau} \cos(w_1 \tau + b_1) \tag{10}$$

The difference between the values of the coefficient b_1 for adjacent blades gives the interblade phase angle. The value of this interblade phase angle for all the nine blades in the cascade is shown in Fig. 5 for both the values of reduced velocity. For $V^* = 9.0$ and 13.0, the average value of interblade phase angle calculated is 320 deg with a standard deviation of 2.1 and 2.4 deg, respectively. Thus it is clear that the time domain method predicts the same value of interblade phase angle as the frequency domain method. It is interesting to observe that the time domain method predicts the phase angle corresponding to the most unstable motion for both stable and unstable motions.

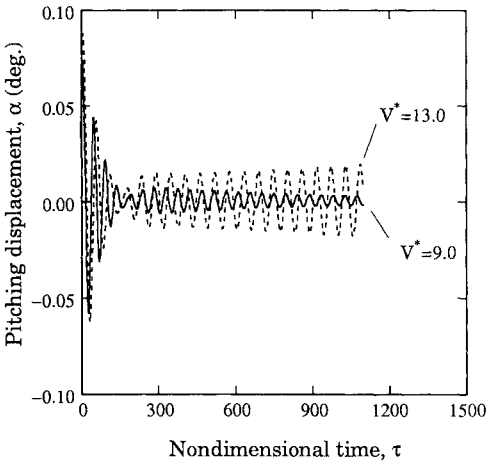

Fig. 4 Second starting procedure, blade motions for reduced velocity $V^* = 9.0$ and 13.0.

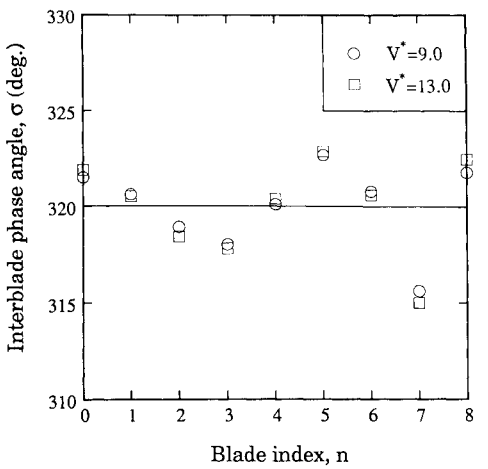

Fig. 5 Calculated values of interblade phase angle σ for reduced velocity $V^* = 9.0$ and 13.0.

The blade-to-blade variation in the phase angle seen in Fig. 5 is a result of the presence of other interblade phase angle modes that have not damped out completely. The choice of initial conditions (small disturbance velocity given to one blade) is such that all interblade phase angle modes are excited initially. As time passes, a redistribution of the energy takes place between the different modes because energy is given to (or taken from) the fluid stream at different rates. The stable modes give up their energy whereas the unstable modes absorb energy. After a very long time, the stable modes will be completely damped out; if all the modes are stable, then the cascade will come to rest. If one mode is unstable, all the motion will be confined to that interblade phase angle mode. It is noted that the time domain solutions simulate experimental observations to the following extent. In both cases, some nonuniformity in the fluid stream results in all phase angle modes being excited, and subsequently the motion of the blades (at flutter) shows some blade-to-blade variation in the interblade phase angle.

The values of the damping coefficient c_1 [in Eq. (10)] obtained for $V^* = 9.0$ and 13.0 are used to linearly interpolate to a condition of neutral stability. The value of reduced velocity at flutter is calculated to be $V^* = 11.9$, and the nondimensional frequency at flutter is found to be $\Omega = 0.118$.

To compare the results at flutter from the time domain and frequency domain methods, the values of reduced velocity V^* and nondimensional frequency Ω are used together with the inlet Mach number M_∞ to calculate the values of reduced frequency $k_c = 0.235$ and frequency ratio $\omega/\omega_\alpha = 1.40$. A comparison with the corresponding values obtained from the frequency domain method, $k_c = 0.238$ and $\omega/\omega_\alpha = 1.33$, shows that the results agree closely. Similarly, the values of reduced frequency $k_c = 0.235$ and frequency ratio $\omega/\omega_\alpha = 1.40$. A comparison with the corresponding values obtained from the frequency domain method, $k_c = 0.238$ and $\omega/\omega_\alpha = 1.33$, shows that the results agree closely. Similarly, the values of reduced frequency k_c and frequency ratio ω/ω_α obtained from the frequency domain method can be used together with the inlet Mach number to calculate the reduced velocity $V^* = 11.2$ and nondimensional frequency $\Omega = 0.119$. Once again, a comparison with the corresponding values from the time domain method, $V^* = 11.9$ and $\Omega = 0.118$, shows good agreement. Table 1 summarizes the results obtained from both the time domain and frequency domain methods for the single-degree-of-freedom example considered here.

All the computations described previously were performed on a Cray X-MP computer. Each of the time domain solutions shown in Fig. 4 required approximately 1800 CPU s; this corresponds to about 90 s per cycle of blade oscillation. For the frequency domain analysis (in which the blades were forced in simple harmonic oscillations), calculations were carried out for three cycles of blade oscillations to allow nonperi-

Table 1 Flutter results for single-degree-of-freedom example (cascade with nine blades)

Parameter	Frequency domain	Time domain
Interblade phase angle σ, deg	320	320
Reduced frequency k_c	0.238	0.235
Frequency ratio ω/ω_α	1.33	1.40
Reduced velocity V^*	11.2	11.9
Nondimensional frequency Ω	0.119	0.118

odic transients to decay. The total computational time for all nine values of phase angle was approximately 1800 s.

Two-Degree-of-Freedom Example

The example considered is a cascade with five blades. The geometric and structural parameters used correspond to the SR5 propfan.[22] The cascade stagger angle θ is 10.7 deg and the gap-to-chord ratio s/c is 1.85. The airfoil section is a NACA 16 series with a thickness-to-chord ratio of 0.03 and a design lift coefficient of 0.3; the Mach number at the inlet section is 0.7. The structural model for each blade is a typical section (pitching and plunging) with elastic axis at the leading edge. The mass ratio is $\mu = 115$ (appropriate for a solid metal blade), the radius of gyration is $r_\alpha = 1.076$, the offset between elastic axis and center of mass is $x_\alpha = 0.964$, and the ratio of uncoupled natural frequencies in bending and torsion is $\omega_h/\omega_\alpha = 0.567$. The grid used in the calculations has 49 points in the streamwise direction and 31 points in the transverse direction in each blade passage; the grid points are distributed nonuniformly in both directions. The nondimensional time step used is 0.1.

A frequency domain solution is obtained as follows. Starting with the steady flowfield, a value of reduced frequency k_c is selected and the airfoils are forced in a plunging motion with a specified interblade phase angle σ until the flowfield becomes periodic in time. The lift and moment coefficients are calculated at each time step and stored; these are later decomposed into Fourier components. This procedure is repeated for pitching motion. In this way, all four frequency domain aerodynamic coefficients [l_{hh}, $l_{h\alpha}$, etc., in Eq. (5)] corresponding to the specified values of reduced frequency, and phase angle are determined. The eigenvalue problem given by Eq. (6) is now solved. The imaginary part of the eigenvalue determines the stability; the system is stable for the selected values of k_c and σ if the imaginary part of both eigenvalues is positive. The preceding steps are then repeated for the remaining values of σ. For a cascade with five blades, the five values of interblade phase angle that can be present at flutter are 0, 72, 144, 216, and 288 deg [see Eq. (7)]. If the cascade is found to be stable at all interblade phase angles, then a lower value of reduced frequency k_c is selected. This is continued until the imaginary part of one of the eigenvalues changes sign (from positive to negative). For the present example, the reduced frequency at flutter is found to be $k_c = 0.225$, the critical phase angle is $\sigma = 288$ deg, and the frequency ratio is $\omega/\omega_\alpha = 0.611$. Figure 6 is a phase plot showing all 10 eigenvalues, 2 for each of the 5 values of phase angle, at $k_c = 0.225$. The phase angles are indicated next to the data points. It can be seen that the eigenvalues fall into two groups. In the group at the lower frequency, the most unstable phase angle is $\sigma = 288$ deg. However, in the other group (at the higher frequency), the interblade phase angle $\sigma = 0$ deg is seen to be equally unstable. Even though the two phase angle modes become unstable at the same value of reduced frequency ($\omega c/M_\infty a_\infty$), the corresponding values of frequency ratio Re$\{\omega/\omega_\alpha\}$ (the ordinate of Fig. 6) differ by more than a factor of 2. Hence, the flutter velocities of the two modes are quite different. The mode corresponding to the lower flutter velocity ($\sigma = 288$ deg) is the more unstable mode as is demonstrated in the following time domain approach.

Next, a time domain solution is obtained for the same example. Only the second starting procedure (described in the previous section) is used in these calculations.

Results are shown for two values of reduced velocity $V^* = 4.8$ and 5.6. Only the center blade is given a small initial pitching velocity α'. All the other blade displacements and velocities are initially zero. Figure 7 shows the variation of the pitching displacement of the center blade with time. The plunging displacement for the center blade, shown in Fig. 8, is seen to have a very similar variation. The displacements of the remaining four blades, not presented here, are initially different due to the unique location of each with respect to the center blade. But beyond $\tau = 200$, the motions of all the blades are similar, except that adjacent blades are displaced along the time axis by an amount corresponding to a phase angle of approximately 288 deg. The displacements h and α of all the blades are curve fit with models of the form given in Eq. (10). The interblade phase angle is calculated as the difference between the values of the phase parameter b_1 for adjacent blades. The average of the phase angle calculated is 288 deg for both $V^* = 4.8$ and 5.6. However, the individual values of the phase angle differ by up to 15 deg from the mean value for $V^* = 4.8$ and up to 9 deg for $V^* = 5.6$. The variation of the phase angle from blade to blade is higher for this case than was observed for the single-degree-of-freedom example. This is because the two values of reduced velocity considered in the present example are very close to the value for neutral stability. Similar calculations made using higher values of reduced velocity, not presented here, show that the variation in the

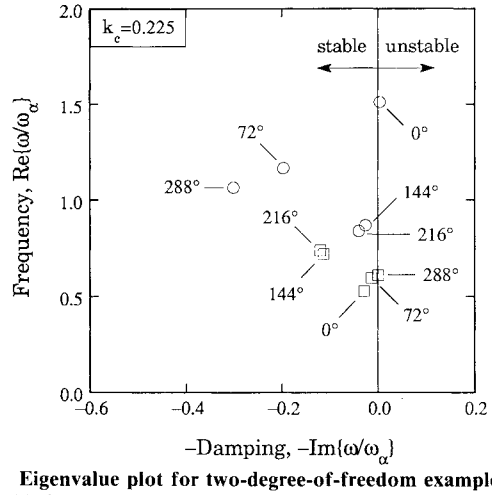

Fig. 6 Eigenvalue plot for two-degree-of-freedom example, values of interblade phase angle as indicated.

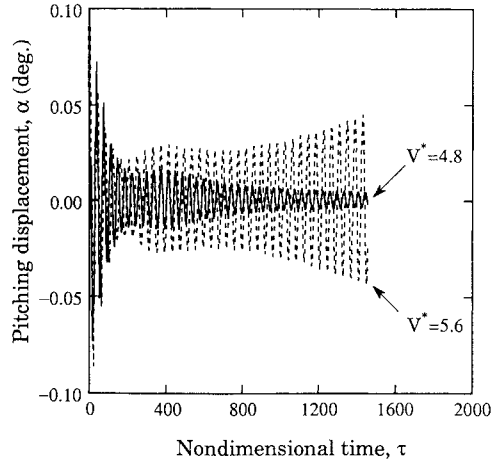

Fig. 7 Pitching displacement for two-degree-of-freedom example, reduced velocity $V^* = 4.8$ and 5.6.

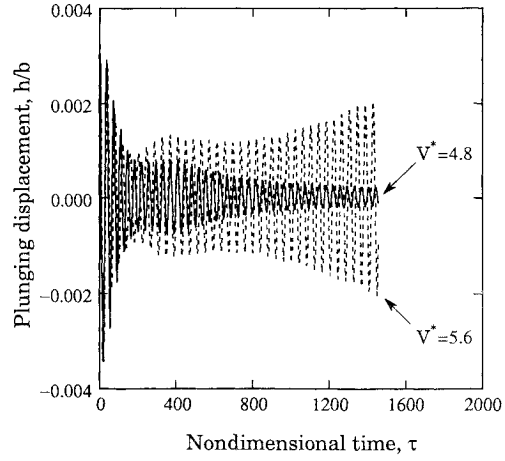

Fig. 8 Plunging displacement for two-degree-of-freedom example, reduced velocity $V^* = 4.8$ and 5.6.

Table 2 Flutter results for two-degrees-of-freedom example (cascade with five blades)

Parameter	Frequency domain	Time domain
Interblade phase angle σ, deg	288	288
Reduced frequency k_c	0.225	0.233
Frequency ratio ω/ω_α	0.611	0.601
Reduced velocity V^*	5.43	5.17
Nondimensional frequency Ω	0.158	0.163
Amplitude ratio $h_0/\alpha_0 b$	2.69	2.76

phase angle (from blade to blade) decreases as the reduced velocity is increased. No significant difference is observed between the phase angles calculated from the pitching and plunging motions.

Once again, it is clear that the time domain method predicts the same value of interblade phase angle as the frequency domain method. The values of the damping coefficient c_1 [in Eq. (10)] obtained for $V^* = 4.8$ and 5.6 are used to interpolate to a condition of neutral stability. The value of reduced velocity at flutter is calculated to be $V^* = 5.17$, and the nondimensional frequency at flutter is found to be $\Omega = 0.163$. A detailed comparison of the results obtained from the time domain and frequency domain methods is shown in Table 2. The comparison reveals good agreement between the results from the two methods.

It must be noted that the frequency domain solution showed two phase angles (288 and 0 deg) becoming unstable at the same reduced frequency. The values of reduced velocity corresponding to these phase angles are 5.43 and 13.4, respectively. The time domain solutions obtained here showed instability at only the phase angle corresponding to the lower value of reduced velocity. It is expected that time domain solutions at the higher values of reduced velocity would contain contributions from both the phase angles. However, the lower value of the reduced velocity is the one of practical interest. Further, it is expected that at such a high value of reduced velocity $V^* = 13.4$ some of the remaining modes may be more unstable as compared to the $\alpha = 0$ deg mode.

Each of the time domain solutions shown in Figs. 7 and 8 required approximately 4000 CPU s on the Cray X-MP; this corresponds to about 100 s per cycle of blade oscillation. For the frequency domain analysis (in which the blades were forced in simple harmonic oscillations), the total computational time required for five values of phase angle and two vibration modes was approximately 2500 s.

Concluding Remarks

A time domain method of flutter analysis has been applied to a cascade. A two-degree-of-freedom typical section model with pitching and plunging motions is used to represent each blade; each blade is allowed to have an independent motion. The aerodynamic model used is based on the two-dimensional, unsteady full-potential equation. The governing aeroelastic equations are integrated in time to obtain the motions of both the fluid and the blades. For purposes of comparison, frequency domain solutions are obtained separately using the same aerodynamic model.

Two examples are used to demonstrate the time domain method. Since the purpose of the calculations is to verify the time domain method, linear examples are selected. In the first example, the typical sections are restricted to only a pitching motion. The phase angle at flutter observed in the frequency domain solutions is accurately reproduced in the time domain solutions. The values of other parameters, such as flutter reduced velocity and flutter reduced frequency, obtained from the frequency and time domain methods show good agreement. In the second example, the typical sections have both pitching and plunging motion. Once again, the results from the two methods are in good agreement.

Even though the examples considered here are linear, the time domain method and the full-potential solver have the capability to model nonlinear behavior in both the structure and flowfield. The full-potential aerodynamic model accounts for actual blade geometry and can be applied to transonic flows containing weak shocks. It should be noted that modern linearized unsteady aerodynamic theories can also account for these effects. Although the structural model used in the present calculations is a simple typical section model, the time domain method can also be used with more advanced structural models obtained from a finite element analysis of three-dimensional configurations.

The time domain method has the capability to fully account for nonlinearities in the aeroelastic model. It can be applied without modification to mistuned systems. It allows a realistic representation of the onset of flutter in a bladed disk when some disturbance is encountered. Because it can deal with finite-amplitude blade motions, the time domain method allows a more complete physical understanding of the cascade flutter phenomenon.

Acknowledgments

This work was funded in part by NASA Lewis Research Center under Grant NSG-3139; George L. Stefko was the monitor. The authors would like to thank Gerald V. Brown and Oral Mehmed of the Structural Dynamics Branch at NASA Lewis Research Center for some helpful discussions and suggestions.

References

[1]Ziemianski, J. A., and Whitlow, J. B., Jr., "NASA/Industry Advanced Turboprop Technology Program," NASA TM-100929, Aug. 1988.

[2]Mehmed, O., Kaza, K. R. V., Lubomski, J. F., and Kielb, R. E., "Bending-Torsion Flutter of a Highly Swept Advanced Turboprop," NASA TM-82975, Oct. 1982.

[3]Bendiksen, O., and Friedmann, P., "Coupled Bending-Torsion Flutter in Cascades," *AIAA Journal,* Vol. 18, No. 2, 1980, pp. 194-201.

[4]Smith, S.N., "Discrete Frequency Sound Generation in Axial Flow Turbomachines," British Aeronautical Research Council, London, ARC R&M 3709, March 1971.

[5]Surampudi, S. P., and Adamczyk, J. J., "Unsteady Transonic Flow Over Cascade Blades," *AIAA Journal,* Vol. 24, No. 2, 1986, pp. 293-302.

[6]Adamczyk, J. J., and Goldstein, M. E., "Unsteady Flow in a Supersonic Cascade with Subsonic Leading-Edge Locus," *AIAA Journal,* Vol. 16, No. 12, 1978, pp. 1248-1254.

[7]Lane, F., "Supersonic Flow Past an Oscillating Cascade with Supersonic Leading-Edge Locus," *Journal of the Aeronautical Sciences,* Vol. 24, Jan. 1957, pp. 65-66.

[8]Atassi, H., and Akai, T. J., "Aerodynamic and Aeroelastic Characteristics of Oscillating Loaded Cascades at Low Mach Number, I. Pressure Distribution, Forces and Moments," *Journal of Engineering for Power,* Vol. 102, No. 2, 1980, pp. 344–351.

[9]Caruthers, J. E., "Aerodynamic Analysis of Cascaded Airfoils in Unsteady Rotational Flow," *Proceedings of the 2nd International Symposium on Aeroelasticity in Turbomachines,* edited by P. Suter, Juris-Verlag, Zurich, Switzerland, 1981, pp. 31–64.

[10]Whitehead, D. S., and Grant, R. J., "Force and Moment Coefficients for High Deflection Cascades," *Proceedings of the 2nd International Symposium on Aeroelasticity in Turbomachines,* edited by P. Suter, Juris-Verlag, Zurich, Switzerland, 1981, pp. 85–127.

[11]Verdon, J. M., and Caspar, J. R., "Development of a Linear Unsteady Aerodynamic Analysis for Finite-Deflection Subsonic Cascades," *AIAA Journal,* Vol. 20, No. 9, 1982, pp. 1259–1267.

[12]Hall, K. C., and Crawley, E. F., "Calculation of Unsteady Flows in Turbmachinery Using the Linearized Euler Equations," *AIAA Journal,* Vol. 27, No. 6, 1989, pp. 777–787.

[13]Verdon, J. M., "Linearized Unsteady Aerodynamic Theory," *AGARD Manual on Aeroelasticity in Axial Flow Turbomachines, Unsteady Turbomachinery Aerodynamics,* Vol. 1, edited by M. F. Platzer and F. O. Carta, AGARD-AG-298, March 1987, Chap. II.

[14]Kao, Y. F., "A Two-Dimensional Unsteady Analysis for Transonic and Supersonic Cascade Flows," Ph.D. Dissertation, School of Aeronautics and Astronautics, Purdue Univ., West Lafayette, IN, May 1989.

[15]Batina, J. T., Bennett, R. M., Seidel, D. A., Cunningham, H. J., and Bland, S. R., "Recent Advances in Transonic Computational Aeroelasticity," *Computers and Structures,* Vol. 30, No. 1/2, 1988, pp. 29–37.

[16]Guruswamy, G. P., "Interaction of Fluids and Structures for Aircraft Applications," *Computers and Structures,* Vol. 30, No. 1/2, 1988, pp. 1–13.

[17]Ballhaus, W. F., and Goorjian, P. M., "Computation of Unsteady Transonic Flows by the Indicial Method," *AIAA Journal,* Vol. 16, No. 2, 1978, pp. 117–124.

[18]Bakhle, M. A., Keith, T. G., Jr., and Kaza, K. R. V., "Application of a Full-Potential Solver to Bending-Torsion Flutter in Cascades," AIAA Paper 89-1386, April 1989.

[19]Lane, F., "System Mode Shapes in the Flutter of Compressor Blade Rows," *Journal of the Aeronautical Sciences,* Vol. 23, Jan. 1956, pp. 54–66.

[20]Bathe, K. J., and Wilson, E. L., *Numerical Methods in Finite Element Analysis,* Prentice-Hall, Englewood Cliffs, NJ, 1976.

[21]Bundas, D. J., and Dugundji, J., "Flutter and Forced Response of Mistuned Rotors Using Standing Wave Analysis," Massachusetts Institute of Technology, Cambridge, MA, GT&PDL Rept. No. 170, March 1983.

[22]Reddy, T. S. R., Srivastava, R., and Kaza, K. R. V., "The Effects of Rotational Flow, Viscosity, Thickness, and Shape on Transonic Flutter Dip Phenomena," AIAA Paper 88-2348, April 1988.

[23]Reddy, T. S. R., Bakhle, M. A., and Huff, D. L., "Flutter Analysis of a Supersonic Cascade in Time Domain Using an Euler Solver," NASA TM, 1991.